Analysis of Current Density and Related Parameters in Spinal Cord Stimulation

Wilbert A. Wesselink, *Student Member, IEEE,* Jan Holsheimer, and Herman B. K. Boom, *Senior Member, IEEE*

***Abstract*— A volume conductor model of the spinal cord and surrounding anatomical structures is used to calculate current (and current density) charge per pulse, and maximum charge density per pulse at the contact surface of the electrode in the dorsal epidural space, in the dorsal columns of the spinal cord and in the dorsal roots. The effects of various contact configurations (mono-, bi-, and tripole), contact area and spacing, pulsewidth and distance between contacts and spinal cord on these electrical parameters were investigated under conditions similar to those in clinical spinal cord stimulation. At the threshold stimulus of a large dorsal column fiber, current density and charge density per pulse at the contact surface were found to be highest ($1.9 \cdot 10^5$ μA/cm^2 and 39.1 μC/cm$^2 \cdot$ p, respectively) when the contact surface was only 0.7 mm^2. When stimulating with a pulse of 500 μs, highest charge per pulse (0.92 μC/p), and the largest charge density per pulse in the dorsal columns (1.59 μC/cm$^2 \cdot$ p) occurred. It is concluded that of all stimulation parameters that can be selected freely, only pulsewidth affects the charge and charge density per pulse in the nervous tissue, whereas both pulsewidth and contact area strongly affect these parameters in the nonnervous tissue neighboring the electrode contacts.**

***Index Terms*—Computer modeling, current density, spinal cord stimulation.**

I. Introduction

SINCE 1967 [1], spinal cord stimulation (SCS) has been used for the management of chronic pain. The rationale for this treatment of chronic pain, using a stimulating electrode in the dorsal epidural space, is based on the "gate control" theory presented by Melzack and Wall [2] in 1965. They theorized that inhibition of small diameter noxious pathways is modulated by the activation of large diameter somatosensory nerve fibers. Suppression of chronic pain can be achieved by stimulation of such large diameter fibers in the dorsal columns of the spinal cord. It is accompanied by paresthesia which may cover the dermatomes corresponding to the spinal cord level of the cathode, and all levels caudally. In SCS, stimulus pulses are typically biphasic, "actively charge balanced," and supplied by a voltage controlled pulse generator connected to one or more longitudinal contact arrays (mono-, bi-, or tripolar) placed in the dorsal epidural space, close to the dura mater [3]. Between the dura mater and the pia mater, surrounding the spinal cord, there is a cerebrospinal fluid (CSF) layer of variable thickness [4].

In clinical practice, SCS electrodes consist of a longitudinal array of contacts of approximately 12 mm^2 active stimulating surface area, separated by 6 mm (edge to edge) [3]. Pulsewidth is typically 210 μs, but may vary from 100 to 500 μs. The therapeutic range of stimulation rates is generally 30–80 pps, while stimulation is applied either continuously or intermittently with duty cycles varying among patients. The stimulation voltage is variable, but related to the perception of paresthesia and to the discomfort threshold, which is generally less than twice the perception threshold [5].

Until now, no data were available regarding the current density distribution in the spinal cord due to epidural stimulation of the spinal cord, neither from experiments, nor from computer modeling. Therefore, the SCS computer model developed by Struijk *et al.* [6]–[9], which calculates the potential field resulting from electrical stimulation, has been extended with an algorithm to calculate current density. This enables the assessment of the current density distribution at each contact surface of the electrode, and in the spinal cord, at a stimulus amplitude corresponding to the activation of the largest superficial nerve fibers in the dorsal columns, which corresponds to the perception threshold of paresthesia.

Charge density per phase and charge per phase are related to current density and total injected current, respectively. Charge per phase is defined as the integral of the current over one phase of the biphasic pulse. Charge density per phase is the charge per phase per unit of contact area bordering the biological tissue, but also the integral of the current density over one phase of the stimulus waveform. Because current density and related parameters ensuing from the stimulation of the spinal cord may depend on several geometrical and other factors, the influence of the anode-cathode configuration, the contact area, the contact spacing, the pulsewidth, and the distance between the contact and the spinal cord were evaluated.

As in electrical stimulation of the brain and peripheral nerves, prolonged SCS may damage (nervous) tissue adjacent to the contact surface. In general, tissue damage owing to electrical stimulation can be ascribed to three separate factors.

1) In peripheral nerve stimulation, nerve fibers may be damaged mechanically as a result of either surgical procedures or mechanical stress from the implanted electrode contacting the nerve, resulting in early nerve fiber degeneration [10]–[12].

Manuscript received February 2, 1996; revised April 16, 1997, January 9, 1998, and March 9, 1998. This work was supported by a grant from Medtronic, Inc., Minneapolis, MN USA.

The authors are with the Institute for Biomedical Technology, University of Twente, 7500 AE Enschede, The Netherlands.

Publisher Item Identifier S 1063-6528(98)03848-8.

TABLE I
COMPARTMENTAL CONDUCTIVITIES [S/m] OF THE VOLUME CONDUCTOR MODEL

gray matter	0.23
white matter	0.60 longitudinal 0.083 transverse
cerebrospinal fluid	1.7
epidural fat	0.04
dura mater	0.03
vertebral bone	0.02
surrounding layer	0.004
electrode insulation	0.002

2) The stimulating current may induce irreversible electrochemical reactions at the contact-tissue interface, producing substances damaging the local nervous tissue [13]–[15].
3) When stimulating at high rates and amplitudes, nervous tissue damage may be related to the prolonged excitation of a large number of nerve cells within a critical volume of tissue (neural hyperactivity) [16], [17]. SCS differs from cortical or deep brain stimulation and peripheral nerve stimulation, because in SCS the nervous tissue is separated from the stimulating electrodes by a rather large volume of continuously circulating CSF. Therefore, any electrochemical reaction at the electrode surface will probably not result in spinal cord damage. The distance between the nervous tissue and the contacts also excludes it from being damaged mechanically. Therefore, any neural tissue damage resulting from SCS should be related to the passing of current through the spinal cord, possibly resulting in neural hyperactivity.

II. METHODS

The SCS computer model, developed at the University of Twente, consists of two parts. The first comprises a three-dimensional cubical cell structure, with cells of variable dimensions. The conductivity of each cell is defined according to the value of the anatomical structure it represents, thus giving rise to an inhomogeneous volume conductor model. The model consists of compartments with specific conductivities, representing the gross anatomy of the spinal cord, e.g. gray and white matter, epidural fat, dura mater, vertebral bone, CSF, and a surrounding border layer representing distant tissues. Anisotropy of the white matter was included by transferring the conductivity matrix onto the orthogonal principal axes and specifying its conductivities along these axes. The dura mater compartment also includes any encapsulation tissue between electrode and dura, and its conductivity was calculated using clinical impedance measurements with a bipolar electrode configuration [8]. The compartmental conductivities used in the UT-SCS model are presented in Table I, and a transverse section of the model at a midcervical spinal level is shown in Fig. 1. Rectangular electrode contacts at the surface of insulating polymer material were modeled dorsomedially in the epidural space next to the dura mater, and, in case of bipolar and tripolar configurations, as a longitudinal array.

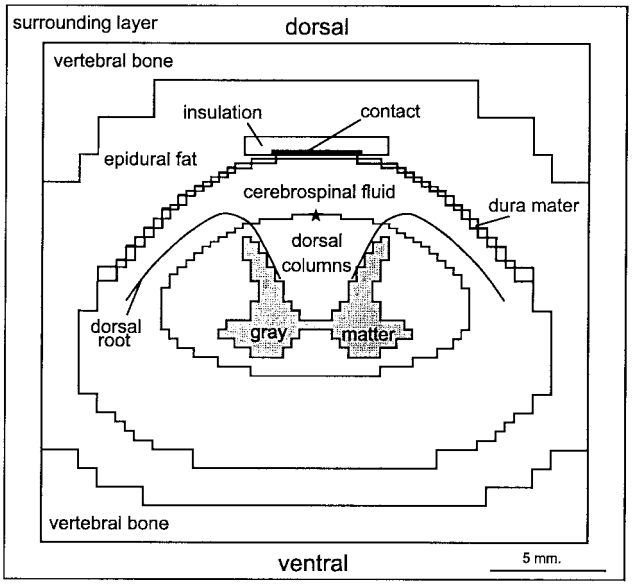

Fig. 1. Transverse section of midcervical spinal cord model; star indicates position of DC fiber on midline of dorsal spinal cord surface.

The steady state potential field, induced by stimulation with constant voltage, was calculated from the discrete form of the Laplace equation. The resulting set of linear equations was solved by a Red–Black Gauss–Seidel iterative method with variable overrelaxation [8]. When monopolar (cathodal) stimulation was modeled, the border of the model served as the distant anode.

The second part of the model describes the electrical response of myelinated nerve fibers to field stimulation, as proposed by McNeal [17]. Instead of the membrane kinetics of frog myelinated nerve, parameters of rabbit nerve fiber membrane, as determined experimentally by Chiu *et al.* [18] were used. These membrane parameters, adapted to body temperature by Struijk *et al.* [7], were implemented to calculate threshold voltages for excitation of mammalian branched dorsal column (DC) fibers and dorsal root (DR) fibers. In the current study, a 12 μm DC fiber with 4 μm collaterals, placed on the midline of the dorsal surface of the spinal cord (see Fig. 1), and a 15 μm DR fiber were used. Threshold voltages for excitation of the DC and the DR fiber were calculated, using a monophasic constant voltage pulse. An extensive description of the UT-SCS computer model has been presented by Struijk *et al.* [6]–[9].

The current density in the spinal cord was determined by calculating its components along the principal axes according to

$$\overleftarrow{J}_x = -\sigma_x \cdot \frac{\partial V}{\partial x} \tag{1}$$

where $\overleftarrow{J}_x$ is the current density component along the x-axis at the point of observation $[\mathrm{A/m^2}]$, σ_x are the material conductivities [S/m] specified along the x-axis of the volume conductor model, and V is the calculated potential [V]. To solve the current density numerically, a finite difference method of first order was used, which maps the continuous equation (1) onto the discrete grid of the inhomogeneous

spinal cord model [19]–[22]. The total electrode current was determined similarly. The specified boundary condition for the electrical potential at the border of the model, i.e., Dirichlet boundary condition, implied that the current perpendicular to the boundary plane was continuous, whereas the other components were zero.

This numerical method to calculate the current density, as well as the program itself, were tested by using a homogeneous, discretized 3-D volume conductor model with a voltage point source at its center and a border layer with a conductivity different from the bulk of the model. The potential in this model was solved numerically, and analytically according to

$$V = \frac{1}{4\pi\sigma} \cdot \frac{I}{r} \tag{2}$$

with V the potential at the point of observation [V], r the distance of this point from the point source [m], I the total current [A], and σ the material conductivity [S/m]. The border layer of the discrete model was given a conductivity such that a good approximation of the infinite extent of the analytical model was obtained, i.e, the potential at the interface of the bulk and the border layer approximated the potential determined analytically. The analytical solution of the current density was determined with (1), using the analytically calculated potential (2), and was compared with the numerical solution. The difference between both solutions of the current density as a function of the distance from the point source did not exceed 5%. Evaluation of the numerical method using a two compartment volume conductor model gave similar results. In order to show current density distributions calculated by the computer model, a routine was implemented to draw iso-current-density lines, connecting points of equal current density in a selected plane of the spinal cord model.

Several SCS related parameters were varied to examine their influence on total electrode current and charge per pulse, and the distribution of current density and charge density per pulse. When a specific parameter was varied, the others were kept at their typical therapeutic standard condition, i.e., contact area: 12.25 mm^2 (3.5 $\times$ 3.5 mm), contact separation (edge-to-edge): 6.5 mm, contact configurations: monopole and longitudinal bipole, and duration of the monophasic, constant voltage pulse: 210 μs. The standard value of the thickness of the CSF layer was 2.4 mm, which is typical for a midcervical spinal cord level [4]. Since the current density at the surface of the rectangular contacts will not be distributed uniformly, the results presented in this study are the maximum current densities, generally present at the corners of the contacts.

III. Results

All presented results are calculated at a stimulation voltage corresponding to the threshold for the excitation of the 12 μm DC fiber on the midline of the dorsal surface of the dorsal columns. In Table II, an overview is presented of the maximum current density (i.e., at the corners of the contact) and the corresponding threshold voltage of the medial 12 μm DC fiber, whereas Table III shows the charge per pulse and the maximum charge density per pulse under the specified conditions for contact configuration, contact area, contact spacing, thickness of the dorsal CSF layer and pulsewidth. The charge per pulse and the maximum charge density per pulse were derived from the total cathodal current and the maximum current density, respectively. The maximum current density and charge density per pulse were calculated at the surface of the cathode, at the border of the dorsal columns, and at a dorsal root at the rostrocaudal level of the cathode.

TABLE II
DC Fiber Threshold Voltages and Related Maximum Current Densities Under Conditions as Specified

Condition	Maximum current density [μA/cm^2]						DC fiber Threshold [V]	
	at corner of contact		in dorsal columns		in dorsal roots			
	mono	bi	mono	bi	mono	bi	mono	bi
12.25 mm^2 contact	$1.7\cdot10^4$	$1.6\cdot10^4$	$2.7\cdot10^3$	$3.2\cdot10^3$	$3.2\cdot10^3$	$2.9\cdot10^3$	1.2	1.8
0.7 mm^2 contact	$1.9\cdot10^5$	$1.8\cdot10^5$	$2.3\cdot10^3$	$2.5\cdot10^3$	$2.4\cdot10^3$	$2.2\cdot10^3$	4.8	8.8
2.5 mm spacing	-	$1.6\cdot10^4$	-	$3.9\cdot10^3$	-	$2.6\cdot10^3$	-	1.7
9.5 mm spacing	-	$1.7\cdot10^4$	-	$3.1\cdot10^3$	-	$3.1\cdot10^3$	-	1.9
1.2 mm CSF	$7.4\cdot10^3$	$7.1\cdot10^3$	$2.5\cdot10^3$	$2.9\cdot10^3$	$2.7\cdot10^3$	$2.4\cdot10^3$	0.6	0.9
3.6 mm CSF	$3.2\cdot10^4$	$3.0\cdot10^4$	$3.0\cdot10^3$	$3.9\cdot10^3$	$3.7\cdot10^3$	$3.5\cdot10^3$	2.2	3.4
10 μs pulsewidth	-	$5.4\cdot10^4$	-	$1.1\cdot10^4$	-	$9.8\cdot10^3$	-	6.2
500 μs pulsewidth	-	$1.6\cdot10^4$	-	$3.2\cdot10^3$	-	$2.9\cdot10^3$	-	1.8

TABLE III
Charge and Maximum Charge Density per Pulse Under Conditions as Specified

Condition	Maximum charge density per pulse [μC/cm^2·p]						Charge per pulse [μC/p]	
	at corner of contact		in dorsal columns		in dorsal roots			
	mono	bi	mono	bi	mono	bi	mono	bi
12.25 mm^2 contact	3.49	3.29	0.56	0.67	0.67	0.60	0.42	0.39
0.7 mm^2 contact	39.08	37.42	0.48	0.53	0.49	0.45	0.28	0.27
2.5 mm spacing	-	3.26	-	0.80	-	0.55	-	0.38
9.5 mm spacing	-	3.51	-	0.65	-	0.65	-	0.42
1.2 mm CSF	1.56	1.50	0.52	0.61	0.56	0.50	0.19	0.18
3.6 mm CSF	6.65	6.21	0.64	0.82	0.78	0.72	0.80	0.74
10 μs pulsewidth	-	0.54	-	0.11	-	0.10	-	0.06
500 μs pulsewidth	-	7.77	-	1.59	-	1.42	-	0.92

A. Effect of the Spinal Cord

The influence of the presence of the spinal cord in the dural sac is shown in Fig. 2(a)–(d). Stimulation was applied monopolarly. 41 iso-current-density lines were drawn ranging from 0 to $8.0 \cdot 10^3$ μA/cm^2 per volt stimulation (0 μA/cm^2 at the corners of the model). Fig. 2(a) is a transverse section of a model where the cord was removed and the dural sac was assumed to be filled with CSF, thus being a homogeneous, well conducting medium surrounded by a rather insulating medium (conductivity ratio 42.5 : 1). In Fig. 2(b) it is shown how the spinal cord affects the distribution of the current. Fig. 2(c) and (d) are midsagittal sections of the models shown in Fig. 2(a) and (b), respectively, as indicated by Y1-Y2 in Fig. 2(a) and (c). The presence of the spinal cord resulted in a deflection of the current near its surface, owing to the low conductivity of the white and gray matter as compared to the CSF (see

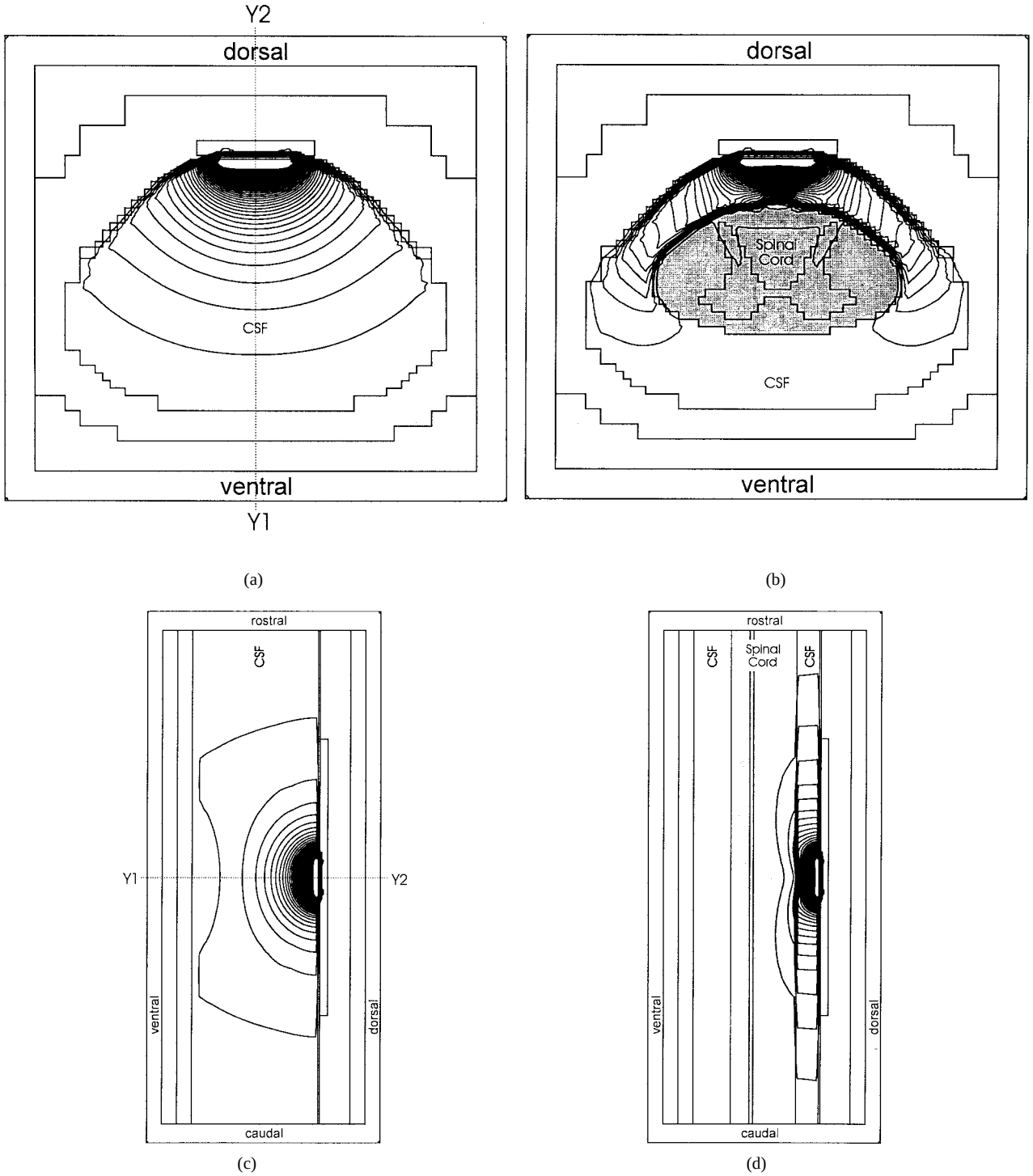

Fig. 2. Transverse [(a) and (b)] and midsagittal sections [(c) and (d)] of midcervical model without [(a) and (c)] and with spinal cord [(b) and (d)] in dural sac (CSF); 41 iso-current-density lines ranging from 0 to 8.0 · 10^3 μA/cm^2 for 1 V stimulus (monopolar).

Table I). Fig. 2(a)–(d) show that without the spinal cord the current density would be distributed rather uniformly in all directions, whereas the presence of the cord will force most current into lateral, rostral and caudal directions through the well conducting CSF. It is shown in Fig. 2(b) and 2(d) that the maximum current density in the spinal cord is not expected to be at a position at the same level as the center of the electrode contact, but a few mm apart in both lateral, and rostro-caudal directions. Moreover, the current density in the spinal cord will only be a fraction (5–10%) of the total current density at the electrode contact(s).

B. Contact Configuration

Fig. 3 shows the maximum charge density and charge per pulse at threshold stimulation of the dorsomedial DC fiber under standard conditions and in monopolar, bipolar, and

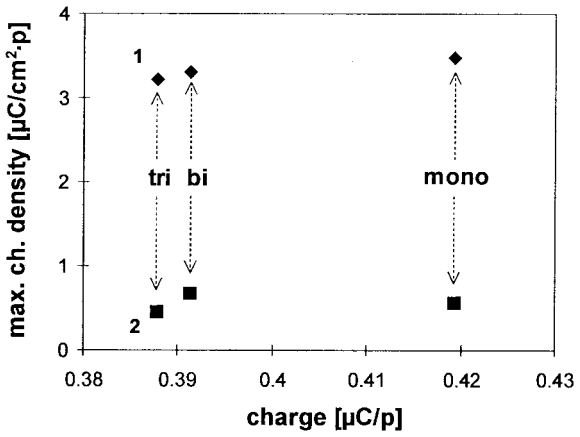

Fig. 3. Calculated charge and maximum charge density per 210 μs pulse for mono-, bi-, and tripolar stimulation: (1) at contact surface, (2) at dorsal border of spinal cord.

tripolar stimulation (the two anodes at both sides of the cathode are at the same potential and give the same current). Data for the monopole and the bipole are given in Tables II and III. Maximum current density appeared at the corners of the rectangular contacts. The charge per pulse required was highest in monopolar stimulation, while ≈7% less charge per pulse was required when the bipole and tripole were used. This result was expected, because bipolar and tripolar configurations have a higher directional selectivity for depolarization of a longitudinal fiber than a monopolar configuration [6]. The maximum charge density per pulse was also highest (≈8%) in monopolar stimulation and 5–7 times higher than at the border of the dorsal columns. At the dorsal roots, the maximum charge density per pulse was 0.5–0.7 μC/cm^2 · p, and differed up to ±17% from the values found at the dorsal column border.

C. Contact Area

Under standard conditions, rectangular contacts of 0.7, 3.15, 7.0, and 12.25 mm^2 were modeled to determine their influence on the maximum current densities at the contact surface, at the border of the spinal cord and at the dorsal roots. As expected, in both mono- and bipolar stimulation, a decrease in contact area resulted in an increase of the required maximum current density at the contact surface, as shown in Fig. 4(a).

Using the monopolar configuration, the maximum current density at the surface of the 0.7 mm^2 contact was approximately 11 times higher than for the 12.25 mm^2 contact (see Table II). Compared to the maximum current density at the dorsal border of the spinal cord, the values at the cathode were 6 and 82 times larger for the 12.25 and 0.7 mm^2 contacts, respectively. At the dorsal column border the maximum current density was highest when the largest contact was used, but it was only 15% less when using the smallest contact. At the dorsal roots, the maximum current density exceeded the values at the dorsal column border by 3 and 17% for the 0.7 and 12.25 mm^2 contacts, respectively. Similar results were computed for the bipolar configuration, as shown in Fig. 4(a) (dashed lines) and Table II.

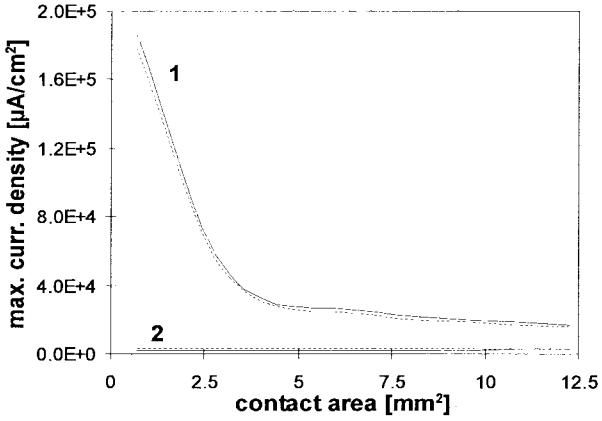

(a)

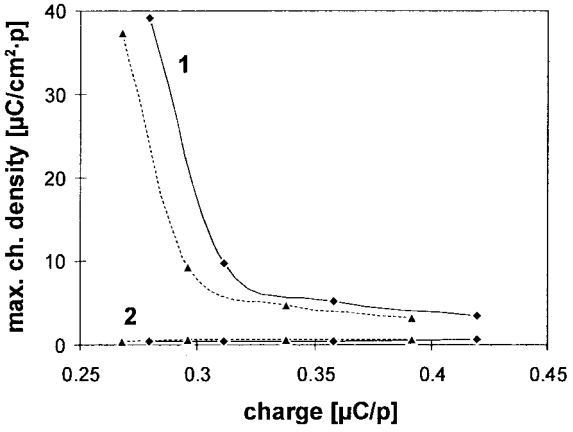

(b)

Fig. 4. Calculated maximum current density (a) and charge and maximum charge density per pulse (b) when varying contact area in monopolar (solid line) and bipolar (dashed line) stimulation: **1** at contact surface and **2** at dorsal border of spinal cord.

Fig. 4(b) shows the corresponding charge per pulse and maximum charge density per pulse for the mono- and bipolar configurations, both at the contact surface and at the border of the spinal cord (see also Table III). Highest charge densities per pulse were found with the smallest contact area. Slightly less charge per pulse was required in bipolar than in monopolar stimulation. For both configurations, the maximum charge density per pulse at the border of the dorsal columns only varied slightly (0.5–0.7 μC/cm^2 · p), and was 5–82 times less than the maximum charge density per pulse at the contact surface.

D. Contact Spacing

The contact spacing of a longitudinal bipolar configuration was varied from 2.5 to 9.5 mm edge-to-edge. The threshold voltage of the DC fiber increased slightly with increasing contact spacing. Maximum current density at the contact surface, the dorsal columns and the dorsal roots did not change much when varying contact spacing (see Table II). The charge per pulse decreased by 10% when reducing the contact spacing from 9.5 to 2.5 mm, whereas the maximum charge density per pulse at the dorsal roots decreased by 15% (see Table III).

E. Thickness of the Dorsal CSF Layer

The thickness of the dorsal CSF layer was varied from 1.2 to 3.6 mm in 0.4 mm steps to determine how the current density distribution would be affected by a varying distance between contacts and spinal cord. When stimulating either monopolarly or bipolarly, an increase of CSF thickness resulted in an increasing current density at the contact(s) of the electrode, whereas the current density at the border of the dorsal columns only varied slightly, as at the dorsal roots.

When stimulating monopolarly, the threshold voltage of the DC fiber increased by a factor 3.7 when the thickness of the CSF layer was increased from 1.2 to 3.6 mm, while the maximum current density at the contact surface became 4.3 times higher (Table II). The ensuing maximum current density in the dorsal columns was 3–10.5 times less than at the contact surface, and increased by only 23% with increasing thickness of the CSF layer. At the dorsal roots, maximum current density was 9–23% higher than in the dorsal columns, and increased by 39% with increasing thickness of the CSF layer. The results of the bipolar configuration were similar (see Table II).

For both configurations, charge per pulse and maximum charge density per pulse related to a varying CSF layer thickness are shown in Fig. 5(a), in which the highest charge density per pulse corresponds with the largest CSF layer (3.6 mm). As expected, the maximum charge density per pulse at the contact surface increased linearly with the charge per pulse. In the dorsal columns the maximum charge density per pulse only varied slightly (approximately 20%) and was 2.5–10.4 times smaller than the maximum charge density per pulse at the contact surface.

F. Pulsewidth

Pulsewidths of 10, 20, 50, 100, 150, 210, 300, and 500 μs were used to determine their influence on charge per pulse and maximum charge density per pulse. An increasing pulsewidth resulted in an increase of both charge and maximum charge density per pulse. At 500 μs pulsewidth the charge (density) per pulse was 14 times higher than at 10 μs, both at the contact surface and in the dorsal columns (Table III). At the contact surface the maximum charge density per pulse was five times higher than in the spinal cord, which was also the ratio of maximum current densities at both sites. As expected, the maximum charge density per pulse increased linearly with increasing charge per pulse at both the contact surface and the border of the spinal cord, as shown in Fig. 5(b). The slope equals the ratio of total current and maximum current density at both sites.

In Fig. 6, the maximum charge density per pulse and the corresponding charge per pulse are shown for all conditions presented in Table III, at a stimulation level of twice the perception threshold. The latter is the lowest of the DC and DR fiber thresholds. Generally, the maximum therapeutic stimulus voltage in SCS is less than twice the perception threshold of paresthesia. The crosses in Fig. 6 represent the results at the electrode contacts, and the values at the border of the dorsal columns are indicated by triangles.

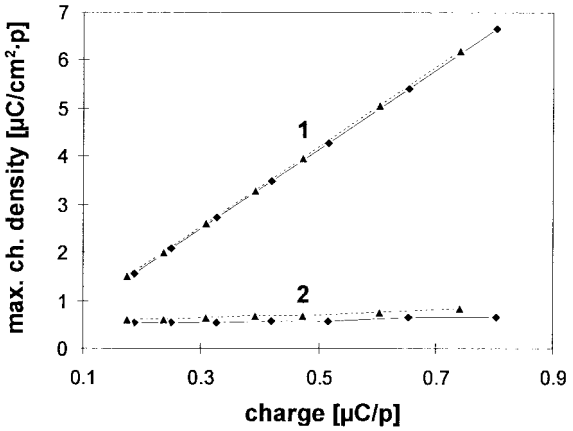

(a)

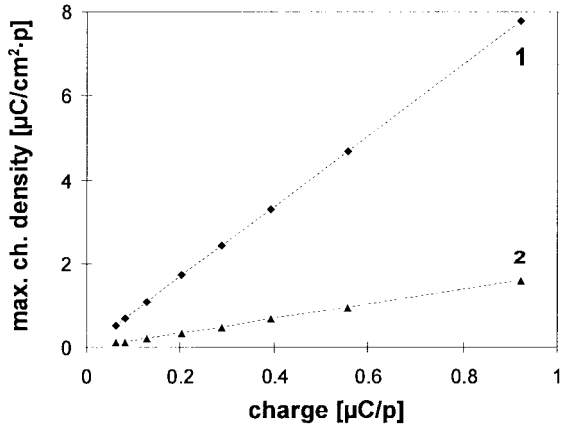

(b)

Fig. 5. Calculated charge and maximum charge density per pulse. (a) varying thickness of CSF layer in monopolar (solid line) and bipolar (dashed line) stimulation: **1** at contact surface and **2** at dorsal border of the spinal cord; thickness of CSF layer (1.2–3.6 mm) increases from left to right. (b) varying pulsewidth in bipolar stimulation: **1** at contact surface and **2** at dorsal border of spinal cord; pulsewidth (10–500 μs) increases from left to right.

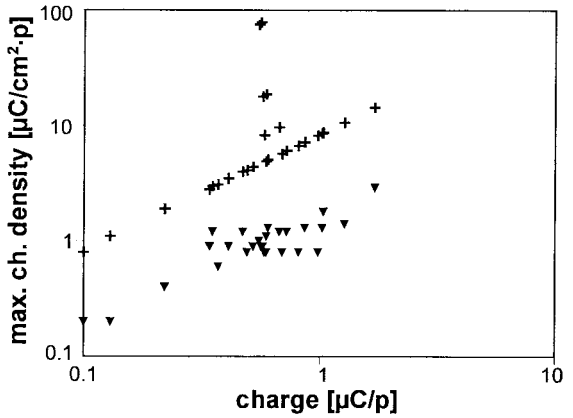

Fig. 6. All calculated data at electrode contact (crosses) and at border of spinal cord (triangles).

IV. Discussion

In this modeling study, the current density distribution in the spinal cord, owing to stimulation with an epidurally placed electrode, was determined with the UT-SCS computer model,

extended with an algorithm to calculate current density. Verification of this algorithm with a homogeneous model showed that it was possible to retrieve an accurate approximation of the current density. Swiontek *et al*. [23] measured current density distributions in the spinal cord of monkeys and human cadavers owing to stimulation at the pia mater. However, we could not use their results to evaluate the calculated current density distributions, because some essential (geometrical) parameters required to model their experiments were lacking. In our model, the presence of a well conducting CSF layer between the (epidural) stimulating electrode and the spinal cord resulted in a different distribution of the stimulating current in the spinal cord. The current density distribution calculated by the computer model confirmed previous statements about the shunting effect of the well conducting CSF layer [6]. Threshold voltages calculated for a typical SCS electrode are within the range of clinically measured voltages [24].

At threshold stimulation of the dorsomedial DC fiber, highest current density and charge density per pulse at the contact surface ($1.9 \cdot 10^5$ μA/cm^2 and 39.1 μC/cm^2 $\cdot$ p, respectively) were found when the contact surface was only 0.7 mm^2. Most charge per pulse (0.92 μC/p) was necessary when stimulating with a pulse of 500 μs. The current density required at the border of the dorsal columns did not change much while varying the contact area, the configuration, the thickness of the CSF layer and the contact spacing, and ranged from $2.3 \cdot 10^3$ to $3.9 \cdot 10^3$ μA/cm^2. Since the low conductivity of the white matter resulted in a deflection of most of the current in the CSF near the surface of the spinal cord [see Fig. 2(b) and (d)], and because of the anisotropy of the white matter (longitudinal conductivity $\approx$9 times higher than transverse conductivity), the small fraction of the current density entering the spinal cord mainly consists of a longitudinal component. The current density at the border of the spinal cord needed for threshold stimulation of the DC fibers is almost independent of the values of the geometrical parameters. An increase of the pulsewidth, however, resulted in an increase of the required charge and charge density per pulse. At a pulsewidth of 500 μs, highest charge per pulse (0.92 μC/p), and the largest charge density per pulse in the dorsal columns (1.59 μC/cm^2 $\cdot$ p) were found.

The dorsal roots were not incorporated in the volume conductor model as separate compartments, because of their small volume compared to the surrounding CSF [9]. Therefore, current density in the dorsal roots was calculated using the conductivity of the CSF. If it is assumed that the conductivity of the dorsal roots equals the (anisotropic) conductivity of the white matter, the current density, and charge density per pulse in the dorsal roots would be at least 3 times less than calculated in this study.

Mechanisms contributing to nervous tissue damage resulting from SCS are not completely understood. Although any neural damage is probably related to the passing of current through the spinal cord, neural hyperactivity, affecting even those nerve fibers not activated by the stimulation, is not expected in SCS. The proportion of large nerve fibers is small and smaller fibers need much larger stimuli [25], resulting in the activation of only a minor part of the nerve fiber population (in contrast to stimulation of the majority of nerve fibers close to the contact in peripheral nerve stimulation [26]).

In recent studies on prolonged peripheral nerve stimulation, McCreery *et al*. [27], [28] introduced the rate of stimulation as a critical parameter for the development of neural damage. The results of these studies might be more relevant to SCS than their previous work on brain cortex [29]. From experiments in which biphasic, charge balanced pulses with a constant pulsewidth (100 μs) were used, they concluded that rates up to 50 pps were safe when using currents recruiting all motor fibers in a peripheral nerve. A mean current ratio of 2.7 for threshold stimulation and full motor fiber recruitment was determined for cuff electrodes (McCreery *et al*. [27]). Although in SCS the ratio of maximum stimulus (discomfort threshold) and perception threshold is usually less than a factor two, pulsewidth and pulse rate may be somewhat higher than in the study by McCreery *et al*. [27], [28]. It is not expected that the pulse rate used in clinical systems would exceed the range presently being used, i.e., 30–80 pps.

Electrochemical reactions at the metal-tissue interface might be the source of chronic inflammation of the fibrous tissue encapsulating the SCS electrode in the epidural space. This effect could lead to further injury or thickening of the capsule and subsequent increase of perception threshold voltage.

It is concluded that of all stimulation parameters that can be selected freely, only pulsewidth affects the charge and charge density per pulse in the nervous tissue. From an electrical safety point of view the pulsewidth should, therefore, not be larger than therapeutically necessary, i.e., less than approximately 300 μs. Moreover, it would not be useful to stimulate with large pulsewidths, because the chronaxie of large spinal myelinated nerve fibers is only 60–90 μs [30]. As for minimum power consumption, the pulsewidth should be approximately 0.2 ms [31]. Both pulsewidth and contact area strongly affect charge and charge density per pulse in the nonnervous tissue neighboring the electrode contacts. A combination of small contact area [less than 3 mm^2, see Fig. 4(a)] and large pulsewidth should be avoided, although each may extend paresthesia coverage and thus the effectiveness of pain management [32], [33].

ACKNOWLEDGMENT

The authors would like to thank J. J. Struijk for his useful discussions and suggestions.

REFERENCES

[1] C. N. Shealy, J. T. Mortimer, and J. B. Reswick, "Electrical inhibition of pain by stimulation of the dorsal columns, preliminary clinical report," *Anesthes. Analges., Curr. Res.*, vol. 46, pp. 489–491, 1967.
[2] R. Melzack and P. D. Wall, *Science, Pain Mechanisms: A New Theory*, vol. 150, pp. 971–979, 1965.
[3] G. Barolat, "Current status of epidural spinal cord stimulation," *Neurosurg. Quart.*, vol. 5, no. 2, pp. 98–124, 1995.
[4] J. Holsheimer, J. A. den Boer, J. J. Struijk, and A. R. Rozeboom, "MR assessment of the normal position of the spinal cord in the spinal canal," *Amer. J. Neuroradiol.*, vol. 15, pp. 951–959, 1994.
[5] J. Holsheimer, "Effectiveness of spinal cord stimulation in the management of chronic pain: Analysis of technical drawbacks and solutions," *Neurosurg.*, vol. 40, pp. 990–996, 1997.
[6] J. J. Struijk, J. Holsheimer, B. K. van Veen, and H. B. K. Boom, "Epidural spinal cord stimulation: Calculation of field potentials with

special reference to dorsal column nerve fibers," *IEEE Trans. Biomed. Eng.*, vol. 38, pp. 104–110, 1991.
[7] J. J. Struijk, J. Holsheimer, G. G. van der Heide, and H. B. K. Boom, "Recruitment of dorsal column fibers in spinal cord stimulation: Influence of collateral branching," *IEEE Trans. Biomed. Eng.*, vol. 39, pp. 903–912, 1992.
[8] J. J. Struijk, J. Holsheimer, G. Barolat, J. He, and H. B. K. Boom, "Paresthesia thresholds in spinal cord stimulation: A comparison of theoretical results with clinical data," *IEEE Trans. Rehab. Eng.*, vol. 1, pp. 101–108, 1993.
[9] J. J. Struijk, J. Holsheimer, and H. B. K. Boom, "Excitation of dorsal root fibers in spinal cord stimulation; A theoretical study," *IEEE Trans. Biomed. Eng.*, vol. 40, pp. 632–639, 1993.
[10] W. Girsch, R. Koller, H. Gruber, J. Holle, C. Liegl, U. Losert, W. Mayr, and H. Thoma, "Histological assessment of nerve lesions caused by epineural electrode application in rat sciatic nerve," *J. Neurosurg.*, vol. 74, pp. 636–642, 1991.
[11] G. G. Naples, J. T. Mortimer, and T. G. H. Yuen, "Overview of peripheral nerve electrode design and implantation," in *Neural Prostheses: Fundamental Studies*. Englewood Cliffs, NJ: Prentice-Hall, chap. 5, pp. 107–146, 1990.
[12] W. F. Agnew, D. B. McCreery, T. G. H. Yuen, and L. A. Bullara, "Histologic and physiologic evaluation of electrically stimulated nerve: Considerations for the selection of parameters," *Ann. Biomed. Eng.*, vol. 17, pp. 39–60, 1989.
[13] ———, "Effects of prolonged electrical stimulation of the central nervous system," in *Neural Prostheses: Fundamental Studies*. Englewood Cliffs, NJ: Prentice-Hall, 1990, chap. 9, pp. 226–230.
[14] L. S. Robblee and T. L. Rose, "Electrochemical guidelines for selection of protocols and electrode materials for neural stimulation," in *Neural Prostheses: Fundamental Studies*. Englewood Cliffs, NJ: Prentice-Hall, 1990, chap. 2, pp. 26–66.
[15] W. F. Agnew and D. B. McCreery, "Considerations for safety with chronically implanted nerve electrodes," *Epilepsia*, vol. 31(suppl.), pp. s27–s32, 1990.
[16] W. F. Agnew, D. B. McCreery, T. G. H. Yuen, and L. A. Bullara, "Local anaesthetic block protects against electrically-induced damage in peripheral nerve," *J. Biomed. Eng.*, vol. 12, pp. 301–308, 1990.
[17] D. R. McNeal, "Analysis of a model for excitation of myelinated nerve," *IEEE Trans. Biomed. Eng.*, vol. BME-23, pp. 329–337, 1976.
[18] S. Y. Chiu, J. M Ritchie, R. B. Rogart, and D. Stagg, "A quantitative description of membrane currents in rabbit myelinated nerve," *J. Physiol.*, vol. 292, pp. 149–166, 1979.
[19] P. J. Dimblow, "Finite difference calculations of current densities in a homogeneous model of a man exposed to extremely low frequency electric fields," *Bioelectromagnet.*, vol. 8, pp. 355–375, 1987.
[20] D. Panescu, J. G. Webster, and R. A. Stratbucker, "Modeling current density distributions during transcutaneous cardiac pacing," *IEEE Trans. Biomed. Eng.*, vol. 41, pp. 549–555, 1994.
[21] F. X. Hart, "Numerical and analytical methods to determine the current density distributions produced in human and rat models by electric and magnetic fields," *Bioelectromagnet.*, suppl. 1, pp. 27–42, 1992.
[22] N. G. Sepulva, J. P. Wikswo, and D. S. Echt, "Finite element analysis of cardiac defibrillation current distributions," *IEEE Trans. Biomed. Eng.*, vol. 37, pp. 354–365, 1990.
[23] T. J. Swiontek, A. Sances, S. J. Larson, J. J. Ackmann, J. F. Cusick, G. A. Meyer, and E. A. Millar, "Spinal cord implant studies," *IEEE Trans. Biomed. Eng.*, vol. BME-23, pp. 307–312, 1976.
[24] G. Barolat, S. Zeme, and B. Ketcik, "Multifactorial analysis of spinal cord stimulation," *Stereotact. Funct. Neurosurg.*, vol. 56, pp. 77–103, 1991.
[25] J. Holsheimer and J. J. Struijk, "How do geometrical factors influence epidural spinal cord stimulation," *Stereotact. Func. Neurosurg.*, vol. 56, pp. 234–249, 1991.
[26] P. H. Veltink, B. K. van Veen, J. J. Struijk, J. Holsheimer, H. B. K. Boom, "A modeling study of nerve fascicle stimulation," *IEEE Trans. Biomed. Eng.*, vol. 36, pp. 683–692, 1989.
[27] D. B. McCreery, W. F. Agnew, T. G. H. Yuen, and L. A. Bullara, "Damage in peripheral nerve from continuous electrical stimulation: Comparison of two stimulation waveforms," *Med. Biol. Eng. Comp.*, vol. 30, pp. 109–114, 1992.
[28] ———, "Relationship between stimulus amplitude, stimulus frequency and neural damage during electrical stimulation of sciatic nerve of cat," *Med. Biol. Eng. Comp.*, vol. 33, pp. 426–429, 1995.
[29] ———, "Charge density and charge per phase as cofactors in the induction of neural injury by electrical stimulation," *IEEE Trans. Biomed. Eng.*, vol. BME-37, pp. 996–1001, 1990.
[30] S. L. Bement and J. B. Ranck, "A quantitative study of electrical stimulation of central myelinated fibers," *Exp. Neurol.*, vol. 24, pp. 147–170, 1969.
[31] D. T. Jobling, R. C. Tallis, E. M. Sedgwick, and L. S. Illis, "Electronic aspects of spinal cord stimulation in multiple sclerosis," *Med. Biol. Eng. Comp.*, vol. 18, pp. 48–56, 1980.
[32] J. Holsheimer, J. J. Struijk, and N. R. Tas, "Effects of electrode geometry and combination on nerve fiber selectivity in spinal cord stimulation," *Med. Biol. Eng. Comp.*, vol. 33, pp. 676–682, 1995.
[33] J .U. Krainick, U. Thoden, and T. Riechert, "Spinal cord stimulation in post-amputation pain," *Surg. Neurol.*, vol. 4, pp. 167–170, 1975.

Wilbert A. Wesselink (S'96) was born in Zelhem, The Netherlands, in 1970. He received the M.Sc. degree in electrical and biomedical engineering from the University of Twente, The Netherlands, in 1994. He is currently working towards the Ph.D. degree at the Institute for Biomedical Technology, University of Twente, Enschede, The Netherlands.

His research is on computer modeling of spinal cord stimulation and the evaluation of clinical studies in which new electrode configurations are applied.

Jan Holsheimer was born in Enschede, The Netherlands, in 1941. He received the M.Sc. degree in biology and biophysics from the University of Groningen, The Netherlands, in 1965 and the Ph.D. degree in biomedical engineering from the University of Twente, Enschede, The Netherlands, in 1982.

In 1965, he joined the Biomedical Engineering Division of the Department of Electrical Engineering at the University of Twente. His primary research interests are the theoretical, experimental and clinical aspects of electrical stimulation of the nervous system. His studies have focused on the design of electrodes enabling the stimulation of specific neuronal pathways as characterized by their positions and fiber diameters.

Herman B. K. Boom (A'89–SM'97) received the Ph.D. degree at the University of Utrecht, The Netherlands, in 1971, where he was trained as a Medical Physicist.

He joined the Department of Medical Physics and Medical Physiology, where he was engaged in research in the field of cardiac mechanics and taught physiology and biophysics. Since 1976, he has been a Professor of Medical Electronics in the Department of Electrical Engineering, University of Twente, Enschede, The Netherlands. His research interests are in cardiovascular system dynamics, bioelectricity, and rehabilitation technology.